



QEX

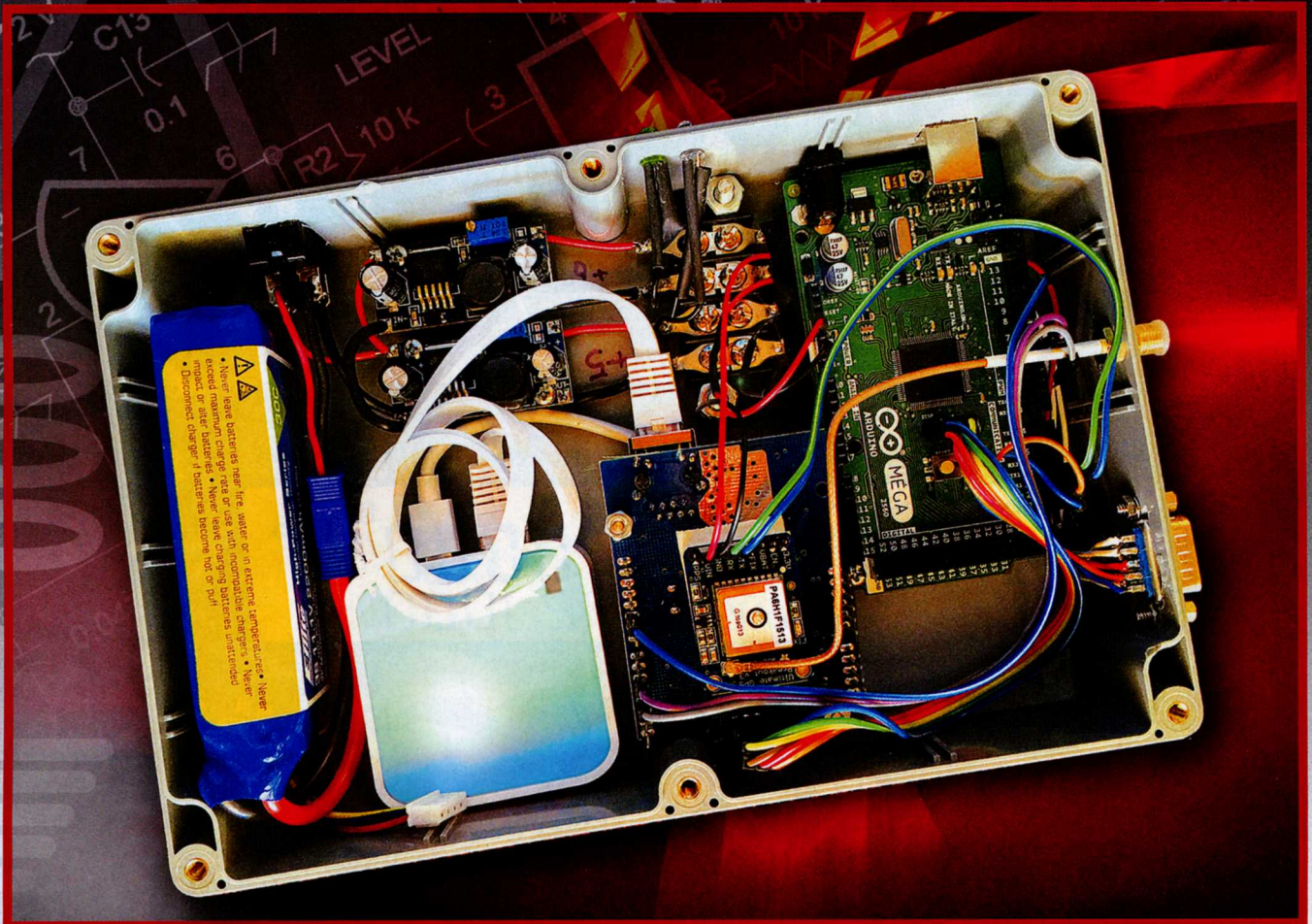
\$5

March/April 2016

www.arrl.org

A Forum for Communications Experimenters

Issue No. 295



WB0EW, shows us how to track Earth orbiting satellites using a two-axis satellite tracker that senses its spatial orientation with respect to Earth's surface, and requires no orientation setup or calibration of any kind.



Calculation of FM and AM Noise Signals of Colpitts Oscillators in the Time Domain

Introduction

An oscillator is a combination of an amplifier, a resonator and phase modulator in a feedback loop. The value of the loop gain and its phase needs to be enough to start oscillation and after the steady state condition maintains oscillation. This is achieved either by voltage or current limiting, by AGC or limiting diodes and is well explained in [1], probably the best explanation of its kind. If such amplitude stabilization would not exist, the amplifier-oscillator would self-destruct. The limiting part of the oscillator keeps the AM (noise) well below the FM noise close-in, but very far-off they reach the same amplitude. Any deviation from this is due to a heavy unwanted non-linearity.

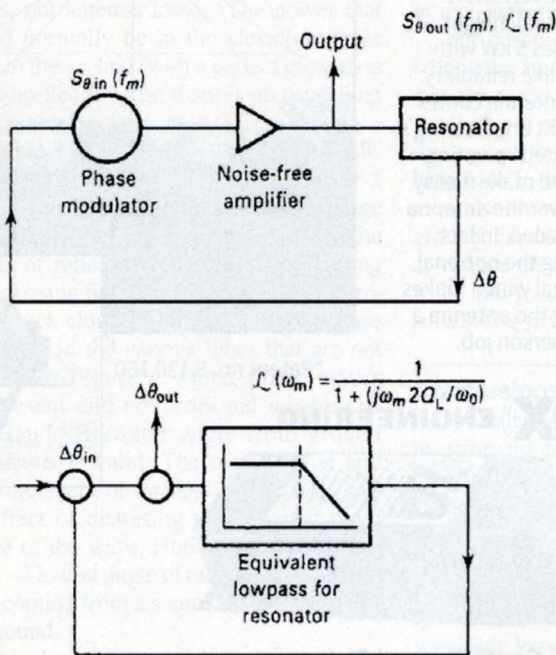


Figure 1 — Block diagram of oscillator and its low pass equivalent based on Leeson's model.

The topic here is to look at the noise of an oscillator.

The oscillator is under large signal condition and also acts like a mixer. Figure 1 shows the block diagram and its low pass equivalent based on Leeson's model [2]. The loop requirement was first mentioned in the Barkhausen analysis [3]. Initial open loop gain for getting started needs to be 3, because the steady state value is approximately 1/3 of the dc transconductance.

The noise has various sources and the following will look at all the steps [4-7]. For the reason of accuracy the

following is a very detailed but complete mathematical analysis.

At the end of this, there will be a set of measurements including details about the results.

In all systems, amplifiers and oscillators, conditions of saturation (specifically with memory effects), tend to amplify AM components.

Noise Generation in Oscillators

As shown above, the qualitative linearized picture of noise generation in oscillators is very well known. The physical effects of random fluctuations taking place in the circuit are different depending on their spectral allocation with respect to the carrier:

Noise components at low frequency deviations result in frequency modulation of the carrier through mean square frequency fluctuation proportional to the available noise power.

Noise components at high frequency deviations result in phase modulation of the carrier through mean square phase fluctuation proportional to the available noise power.

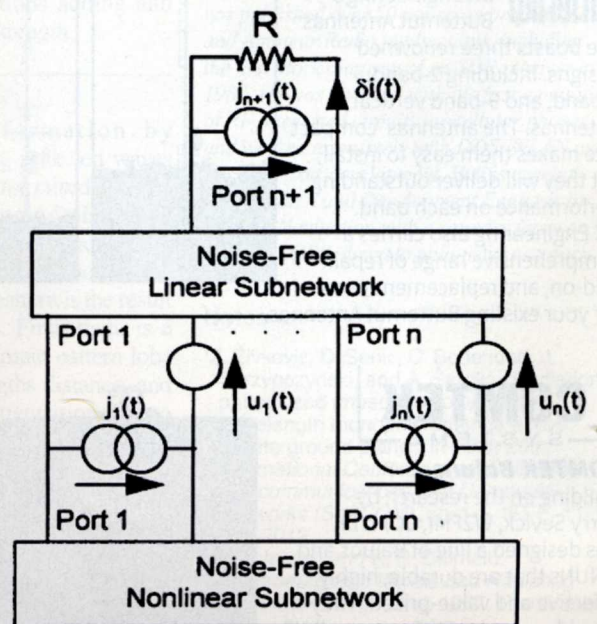


Figure 2 — Equivalent circuit of a general noisy nonlinear network

We will demonstrate that the same conclusions can be quantitatively derived from the HB equations for an autonomous circuit [5, 8].

Equivalent Representation of a Noisy Nonlinear Circuit

A general noisy nonlinear network can be described by the equivalent circuit shown in Figure 2. The circuit is divided into linear and nonlinear subnetworks as noise-free multi-ports. Noise generation is accounted for by connecting a set of noise voltage and noise current sources at the ports of the linear subnetwork [9-11].

Frequency Conversion Approach

The circuit supports a large-signal time periodic steady state of fundamental angular frequency ω_0 (carrier). Noise signals are small perturbations superimposed on the steady state, represented by families of pseudo-sinusoids located at the sidebands of the carrier harmonics. Therefore, the noise performance of the circuit is determined by the exchange of the power among the sidebands of the unperturbed steady state through frequency conversion in the nonlinear subnetwork. Due to the perturbative assumption, the nonlinear subnetwork can be replaced with a multi-frequency linear multi-port described by a conversion matrix. The flow of noise signals can be computed by means of conventional linear circuit techniques.

The frequency conversion approach frequently used has the following limitations:

The frequency conversion approach is not sufficient to predict the noise performance of an autonomous circuit. The spectral density of the output noise power, and consequently the PM noise computed by the conversion analysis are proportional to the available power of the noise sources.

- In the presence of both thermal and flicker noise sources, PM noise increases: as ω^{-1} for $\omega \rightarrow 0$; tends to a finite limit for $\omega \rightarrow \infty$.
- Frequency conversion analysis correctly predicts the far carrier noise behavior of an oscillator, and in particular the oscillator noise floor; does not provide results consistent with the physical observations at low deviations from the carrier.

This inconsistency can be removed by adding the modulation noise analysis. In order to determine the far away noise using the autonomous circuit perturbation analysis, the following applies.

The circuit supports a large-signal time-periodic autonomous regime. The circuit is perturbed by a set of small sources located at the carrier harmonics and at the sidebands at a deviation ω from carrier harmonics. The perturbation of the circuit state ($\delta X_B, \delta X_H$) is given by the uncoupled sets of equations,

$$\frac{\partial E_B}{\partial E_B} \delta X_B = J_B(\omega) \quad (1)$$

$$\frac{\partial E_H}{\partial E_H} \delta X_H = J_H(\omega) \quad (2)$$

where,

E_B, E_H = vectors of HB errors

X_B, X_H = vectors of state variable (SV) harmonics (since the circuit is autonomous, one of the entries X is replaced by the fundamental frequency ω_0)

J_B, J_H = vectors of forcing terms

The subscripts B and H denote sidebands and carrier harmonics, respectively.

For a spot noise analysis at a frequency ω , the noise sources can be interpreted in either of two ways:

- Pseudo-sinusoids with random amplitude and phase located at the sidebands. Noise generation is described by Equation (1) which is essentially a frequency conversion equation relating the sideband harmonics of the state variables and of the noise sources. This description is exactly equivalent to the one provided by the frequency conversion approach. This mechanism is referred to as *conversion noise* [12-15].

Sinusoids located at the carrier harmonics are randomly phase-and-amplitude-modulated by pseudo-sinusoidal noise at frequency ω . Noise generation is described by Equation (2), which describes noise-induced jitter of the circuit-state, represented by the vector δX_H . The modulated perturbing signals are represented by replacing the entries of J_H with the complex modulation laws. This mechanism is referred to as *modulation noise*. One of the entries of δX_H is $\delta\omega_0$ where $\delta\omega_0(\omega) =$ phasor of the pseudo-sinusoidal components of the fundamental frequency fluctuations in a 1 Hz band at frequency ω . Equation (2) provides a frequency jitter with a mean square value proportional to the available noise power. In the presence of both thermal and flicker noise, PM noise raises as ω^{-3} for $\omega \rightarrow 0$ and tends to 0 for $\omega \rightarrow \infty$. Modulation noise analysis correctly describes the noise behavior of an oscillator at low deviations from the carrier and does not provide results consistent with physical observations at high deviations from the carrier.

The combination of both phenomena explains the noise in the oscillator shown in Figure 3, where the near carrier noise dominates below ω_X and far carrier noise dominates above ω_X .

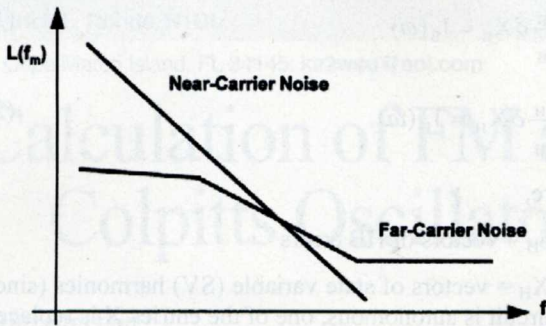


Figure 3 — Oscillator noise components.

Figure 4 (itemized form) shows the noise sources as they are applied at the IF. We have arbitrarily defined the low oscillator output as IF. This applies to the conversion matrix calculation.

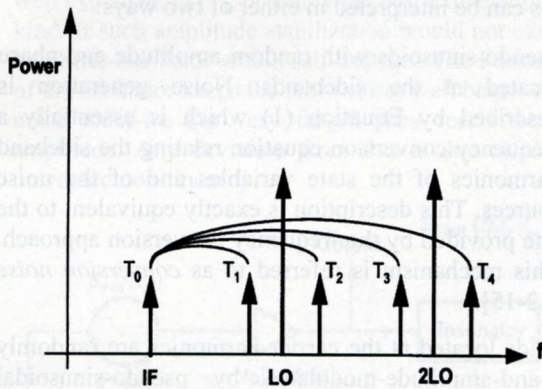


Figure 4 — Noise sources where the noise at each sideband contributes to the output noise at the IF through frequency conversion.

Figure 5 shows the total contributions which have to be taken into consideration for calculation of the noise at the output. The accuracy of the calculation of the phase noise depends highly on the quality of the parameter extraction for the nonlinear device; in particular, high frequency phenomena must be properly modeled. In addition, the flicker noise contribution is essential. This is also valid for mixer noise analysis.

Conversion Noise Analysis

The actual mathematics used to calculate the noise result (Ansoft Serenade 8.x) is as follows [19],

k^{th} harmonic PM noise:

$$\langle \delta\Phi_k(\omega) \rangle^2 = \frac{N_k(\omega) - N_{-k}(\omega) - 2 \operatorname{Re}[C_k(\omega)]}{R |I_k^{SS}|^2} \quad (3)$$

k^{th} harmonic AM noise:

$$\langle \delta A_k(\omega) \rangle^2 = 2 \frac{N_k(\omega) - N_{-k}(\omega) + 2 \operatorname{Re}[C_k(\omega)]}{R |I_k^{SS}|^2} \quad (4)$$

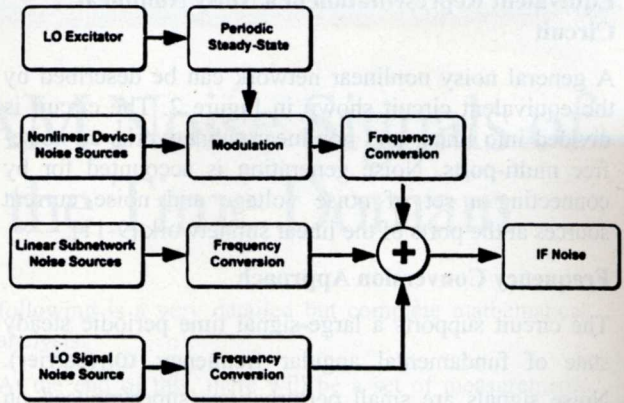


Figure 5 — Noise mechanisms.

k^{th} harmonic PM-AM correlation coefficient:

$$C_k^{PMAM}(\omega) = \langle \delta\Phi_k(\omega) \delta A_k(\omega) \rangle \langle \delta\Phi_k(\omega) \delta A_k(\omega) \rangle^{-1/2} \\ = -\sqrt{2} \frac{2 \operatorname{Im}[C_k(\omega)] + j[N_k(\omega) - N_{-k}(\omega)]}{R |I_k^{SS}|^2} \quad (5)$$

where

$N_k(\omega), N_{-k}(\omega)$ = noise power spectral densities at the upper and lower sidebands of the k^{th} harmonic

$C_k(\omega)$ = normalized correlation coefficient of the upper and lower sidebands of the k^{th} carrier harmonic

R = load resistance

I_k^{SS} = k^{th} harmonic of the steady-state current through the load.

Modulation Noise Analysis

k^{th} harmonic PM noise:

$$\langle \delta\Phi_k(\omega) \rangle^2 = \frac{k^2}{\omega^2} \mathbf{T}_F \rangle \mathbf{J}_H(\omega) \mathbf{J}_H^t(\omega) \langle \mathbf{T}_F^t \quad (6)$$

k^{th} harmonic AM noise:

$$\langle \delta A_k(\omega) \rangle^2 = \frac{2}{|I_k^{SS}|^2} \mathbf{T}_{Ak} \rangle \mathbf{J}_H(\omega) \mathbf{J}_H^t(\omega) \langle \mathbf{T}_{Ak}^t \quad (7)$$

k^{th} harmonic PM-AM correlation coefficient:

$$C_k^{PMAM}(\omega) = \langle \delta\Phi_k(\omega) \delta A_k(\omega) \rangle \langle \delta\Phi_k(\omega) \delta A_k(\omega) \rangle^{-1/2} \\ = \frac{k \sqrt{2}}{j \omega |I_k^{SS}|^2} \mathbf{T}_F \rangle \mathbf{J}_H(\omega) \mathbf{J}_H^t(\omega) \langle \mathbf{T}_{Ak}^t \quad (8)$$

where

$\mathbf{J}_H(\omega)$ = vector of Norton equivalent of the noise sources

\mathbf{T}_F = frequency transfer matrix

R = load resistance

$I_k^{ss} = k^{\text{th}}$ harmonic of the steady-state current through the load.

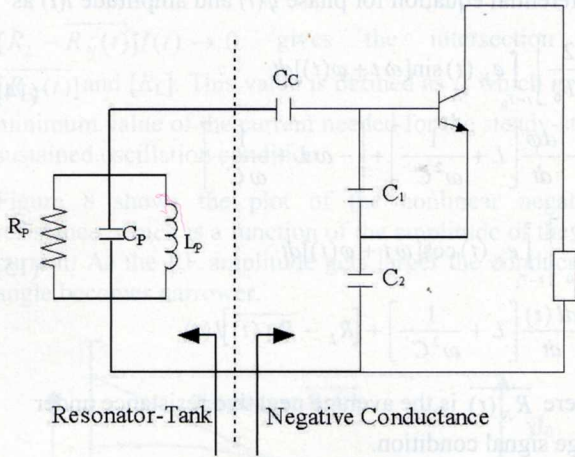


Figure 6 — Colpitts Oscillator configuration for the intrinsic case, no parasitics assumed, and an ideal transistor considered.

The following two circuits show the transition from a series tuned circuit connected with the series time-dependent negative resistance and the resulting input capacitance marked C_{IN} . Translated, the resulting configuration consists of a series circuit with inductance L and the resulting capacitance C' . The noise voltage $e_N(t)$ describes a small perturbation, which is the noise resulting from R_L and $-R_N(t)$. Figure 7 shows the equivalent representation of the oscillator circuit in the presence of noise.

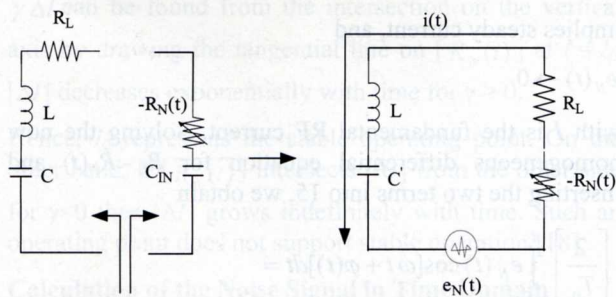


Figure 7 — Equivalent representation of the oscillator circuit in presence of noise.

The circuit equation of the oscillator circuit of Figure 7 can be given as

$$L \frac{di(t)}{dt} + (R_L - R_N(t))i(t) + \frac{1}{C'} \int i(t) dt = e_N(t) \quad (9)$$

where $i(t)$ is the time varying resultant current. Due to the noise voltage $e_N(t)$, Equation (9) is a nonhomogeneous differential equation. If the noise voltage is zero, it translates into a homogeneous differential equation.

For a noiseless oscillator, the noise signal $e_N(t)$ is zero and the expression of the free-running oscillator current $i(t)$ can be assumed to be a periodic function of time and can be given as

$$i(t) = I_1 \cos(\omega t + \varphi_1) + I_2 \cos(2\omega t + \varphi_2) \quad (10)$$

$$+ I_3 \cos(3\omega t + \varphi_3) + \dots + I_n \cos(n\omega t + \varphi_n)$$

where I_1, I_2, \dots, I_n are peak harmonic amplitudes of the current and $\varphi_1, \varphi_2, \dots, \varphi_n$ are time invariant phases.

In the presence of the noise perturbation $e_N(t)$, the current $i(t)$ may no longer be a periodic function of time and can be expressed as

$$i(t) = I_1(t) \cos[\omega t + \varphi_1(t)] + I_2(t) \cos[2\omega t + \varphi_2(t)] + \quad (11)$$

$$I_3(t) \cos[3\omega t + \varphi_3(t)] + \dots + I_{n-2}(t) \cos[(n-2)\omega t + \varphi_{n-2}(t)] +$$

$$I_{n-1}(t) \cos[(n-1)\omega t + \varphi_{n-1}(t)] + I_n(t) \cos[n\omega t + \varphi_n(t)]$$

where $I_1(t), I_2(t), \dots, I_n(t)$ are time variant amplitudes of the current and $\varphi_1(t), \varphi_2(t), \dots, \varphi_n(t)$ are time variant phases.

Considering that $I_n(t)$ and $\varphi_n(t)$ do not change much over the period of $2\pi/n\omega$; each corresponding harmonic over one period of oscillation cycle remains small and more or less invariant. The solution of the differential equation becomes easy since the harmonics are suppressed due to a $Q > 10$, which prevents $i(t)$ to flow for the higher terms.

After the substitution of the value of $\frac{di}{dt}$ and $\int i(t) dt$, the complete oscillator circuit equation, as given in Equation (9), can be rewritten as

$$L \left\{ \begin{aligned} & -I_1(t) \left(\omega + \frac{d\varphi_1(t)}{dt} \right) \sin[\omega t + \varphi_1(t)] + \frac{dI_1(t)}{dt} \cos[\omega t + \varphi_1(t)] + \\ & -I_2(t) \left(2\omega + \frac{d\varphi_2(t)}{dt} \right) \sin[2\omega t + \varphi_2(t)] + \frac{dI_2(t)}{dt} \cos[2\omega t + \varphi_2(t)] + \\ & -I_3(t) \left(3\omega + \frac{d\varphi_3(t)}{dt} \right) \sin[3\omega t + \varphi_3(t)] + \frac{dI_3(t)}{dt} \cos[3\omega t + \varphi_3(t)] + \dots \\ & -I_n(t) \left(n\omega + \frac{d\varphi_n(t)}{dt} \right) \sin[n\omega t + \varphi_n(t)] + \frac{dI_n(t)}{dt} \cos[n\omega t + \varphi_n(t)] \end{aligned} \right\} + [(R_L - R_N(t))i(t)] +$$

$$\begin{aligned}
& \frac{1}{C'} \left\{ \left[\frac{I_1(t)}{\omega} - \frac{I_1(t)}{\omega^2} \left(\frac{d\varphi_1(t)}{dt} \right) \right] \sin[\omega t + \varphi_1(t)] + \right. \\
& \left. \frac{1}{\omega^2} \left(\frac{dI_1(t)}{dt} \right) \cos[\omega t + \varphi_1(t)] \right\} + \\
& \frac{1}{C'} \left\{ \left[\frac{I_2(t)}{2\omega} - \frac{I_2(t)}{4\omega^2} \left(\frac{d\varphi_2(t)}{dt} \right) \right] \sin[2\omega t + \varphi_2(t)] \right. \\
& \left. + \frac{1}{4\omega^2} \left(\frac{dI_2(t)}{dt} \right) \cos[2\omega t + \varphi_2(t)] \right\} + \\
& \frac{1}{C'} \left\{ \left[\frac{I_3(t)}{3\omega} - \frac{I_3(t)}{9\omega^2} \left(\frac{d\varphi_3(t)}{dt} \right) \right] \sin[3\omega t + \varphi_3(t)] + \right. \\
& \left. \frac{1}{9\omega^2} \left(\frac{dI_3(t)}{dt} \right) \cos[3\omega t + \varphi_3(t)] \right\} + \dots \\
& \frac{1}{C'} \left\{ \left[\frac{I_n(t)}{n\omega} - \frac{I_n(t)}{n^2\omega^2} \left(\frac{d\varphi_n(t)}{dt} \right) \right] \sin[n\omega t + \varphi_n(t)] \right. \\
& \left. + \frac{1}{n^2\omega^2} \left(\frac{dI_n(t)}{dt} \right) \cos[n\omega t + \varphi_n(t)] \right\} = e_N(t) \quad (12)
\end{aligned}$$

Because $Q > 10$ we approximate:

$$\begin{aligned}
\frac{di(t)}{dt} &= -I_1(t) \left(\omega + \frac{d\varphi_1(t)}{dt} \right) \sin[\omega t + \varphi_1(t)] \\
&+ \frac{dI_1(t)}{dt} \cos[\omega t + \varphi_1(t)] + \\
&+ (\text{a slowly varying function at higher order harmonics of a very small amount}).
\end{aligned}$$

$$\begin{aligned}
\int i(t) dt &= \left[\frac{I_1(t)}{\omega} - \frac{I_1(t)}{\omega^2} \left(\frac{d\varphi_1(t)}{dt} \right) \right] \sin[\omega t + \varphi_1(t)] \\
&+ \frac{1}{\omega^2} \left(\frac{dI_1(t)}{dt} \right) \cos[\omega t + \varphi_1(t)] + \\
&+ (\text{a slowly varying function at higher order harmonics of a very small amount}).
\end{aligned}$$

After the substitution of the value of di/dt and $\int i(t) dt$, the oscillator circuit Equation (12) can be rewritten as

$$\begin{aligned}
L \left[\begin{aligned} & -I_1(t) \left(\omega + \frac{d\varphi_1(t)}{dt} \right) \sin[\omega t + \varphi_1(t)] \\ & + \frac{dI_1(t)}{dt} \cos[\omega t + \varphi_1(t)] \end{aligned} \right] + [R_L - \overline{R_N(t)}] I(t) + \\
\frac{1}{C} \left\{ \left[\frac{I_1(t)}{\omega} - \frac{I_1(t)}{\omega^2} \left(\frac{d\varphi_1(t)}{dt} \right) \right] \sin[\omega t + \varphi_1(t)] \right. \\
\left. + \frac{1}{\omega^2} \left(\frac{dI_1(t)}{dt} \right) \cos[\omega t + \varphi_1(t)] \right\} = e_N(t) \quad (13)
\end{aligned}$$

Following [18], and for simplification purposes, the equations above are multiplied with $\sin[\omega t + \varphi_1(t)]$ or

$\cos[\omega t + \varphi_1(t)]$ and integrated over one period of the oscillation cycle, which will give an approximate differential equation for phase $\varphi(t)$ and amplitude $i(t)$ as

$$\begin{aligned}
& \left[\frac{2}{T_0} \right] \int_{t-T_0}^t e_N(t) \sin[\omega t + \varphi(t)] dt \\
& = -\frac{d\varphi}{dt} \left[L + \frac{1}{\omega^2 C'} \right] + \left[-\omega L + \frac{1}{\omega C'} \right]
\end{aligned} \quad (14)$$

$$\begin{aligned}
& \left[\frac{2}{T_0} \right] \int_{t-T_0}^t e_N(t) \cos[\omega t + \varphi(t)] dt \\
& = \frac{dI(t)}{dt} \left[L + \frac{1}{\omega^2 C'} \right] + [R_L - \overline{R_N(t)}] I(t)
\end{aligned} \quad (15)$$

where $\overline{R_N(t)}$ is the average negative resistance under large signal condition.

$$\overline{R_N(t)} = \left[\frac{2}{T_0 I} \right] \int_{t-T_0}^t R_N(t) I(t) \cos^2[\omega t + \varphi(t)] dt \quad (16)$$

Since the magnitude of the higher harmonics are not significant, the subscript of $\varphi(t)$ and $I(t)$ are dropped. Based on [18], we now determine the negative resistance.

Calculation of the Region of the Nonlinear Negative Resistance

Under steady-state free running oscillation condition,

$$\frac{dI(t)}{dt} \rightarrow 0$$

implies steady current, and

$$e_N(t) \rightarrow 0$$

with I is the fundamental RF current. Solving the now homogeneous differential equation for $R_L - \overline{R_N(t)}$ and inserting the two terms into 15, we obtain

$$\left[\frac{2}{T_0} \right] \int_{t-T_0}^t e_N(t) \cos[\omega t + \varphi(t)] dt = \quad (17)$$

$$\frac{dI}{dt} \left[L + \frac{1}{\omega^2 C'} \right] + [R_L - \overline{R_N(t)}] I(t)$$

term $\rightarrow 0$

now we introduce

$$\gamma; \quad \gamma = \Delta R / \Delta I; \quad \text{for } \Delta \rightarrow 0, \gamma \rightarrow 0$$

$$\text{and } [R_L - \overline{R_N(t)}] = \gamma \Delta I$$

$$\gamma \rightarrow 0 \Rightarrow [R_L - \overline{R_N(t)}] I(t) \rightarrow 0 \quad (18)$$

$$R_L - \overline{R_N(t)} = R_{Load} - \left[\frac{2}{T_0} \int_{t-T_0}^t R_N(t) \cos^2[\omega t + \varphi(t)] dt \right] \rightarrow 0 \quad (19)$$

$[R_L - \overline{R_N(t)}]I(t) \rightarrow 0$ gives the intersection of $[\overline{R_N(t)}]$ and $[R_L]$. This value is defined as I_0 which is the minimum value of the current needed for the steady-state sustained oscillation condition.

Figure 8 shows the plot of the nonlinear negative resistance, which is a function of the amplitude of the RF current. As the RF amplitude gets larger the conducting angle becomes narrower.

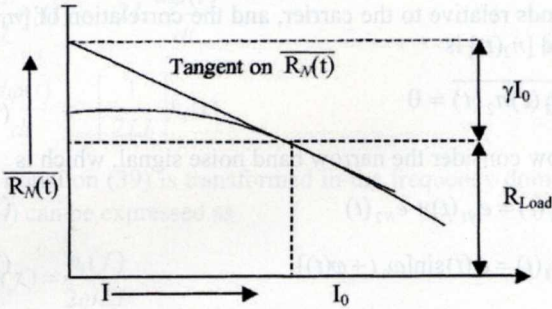


Figure 8 — Plot of negative resistance of $[\overline{R_N(t)}]$ vs. amplitude of current I .

For a small variation of the current ΔI from I_0 , the relation above is expressed as

$$[R_L - \overline{R_N(t)}] = \gamma \Delta I \quad (20)$$

$\gamma \Delta I$ can be found from the intersection on the vertical axis by drawing the tangential line on $[\overline{R_N(t)}]$ at $I = I_0$. $|\Delta I|$ decreases exponentially with time for $\gamma > 0$.

Hence, I_0 represents the stable operating point. On the other hand, if $[\overline{R_N(t)}]$ intersects $[R_L]$ from the other side for $\gamma < 0$ then $|\Delta I|$ grows indefinitely with time. Such an operating point does not support stable operation [18].

Calculation of the Noise Signal in Time Domain

From solving the two orthogonal equations, we need to obtain information about current $I(t)$ and $\varphi(t)$.

$$\begin{aligned} & \left[\frac{2}{IT_0} \int_{t-T_0}^t e_N(t) \sin[\omega t + \varphi(t)] dt \right] \\ &= -\frac{d\varphi(t)}{dt} \left[L + \frac{1}{\omega^2 C'} \right] + \left[-\omega L + \frac{1}{\omega C'} \right] \end{aligned} \quad (21)$$

$$\begin{aligned} & \left[\frac{2}{T_0} \int_{t-T_0}^t e_N(t) \cos[\omega t + \varphi(t)] dt \right] \\ &= \frac{dI(t)}{dt} \left[L + \frac{1}{\omega^2 C'} \right] + [R_L - \overline{R_N(t)}]I(t) \end{aligned} \quad (22)$$

The analysis of the noise signal can be accomplished by decomposing the noise signal $e_N(t)$ to an infinite number of random noise pulses represented by

$$\varepsilon \delta(t - t_0) \quad (23)$$

where ε is the strength of the pulse at the time instant t_0 , and both ε and t_0 are independent random variables from one pulse to next pulse!

The time average of the square of the current pulses over a period of time can be shown to be

$$\frac{1}{2T} \int_{-T}^T [\sum \varepsilon \delta(t - t_0)]^2 dt = \overline{e_N^2(t)} \quad (24)$$

The mean square noise voltage $\overline{e_N^2(t)}$ is generated in the circuit in Figure 7.

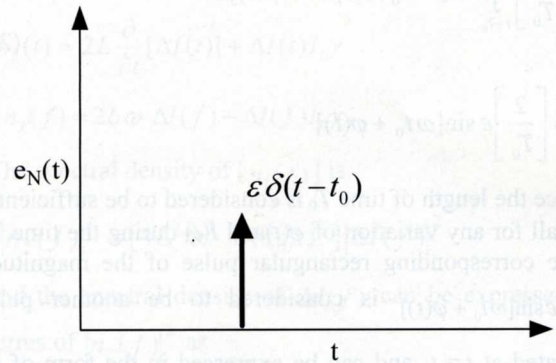


Figure 9 — The noise pulse at $I = I_0$.

Figure 9 shows the noise pulse at time instant $t = t_0$.

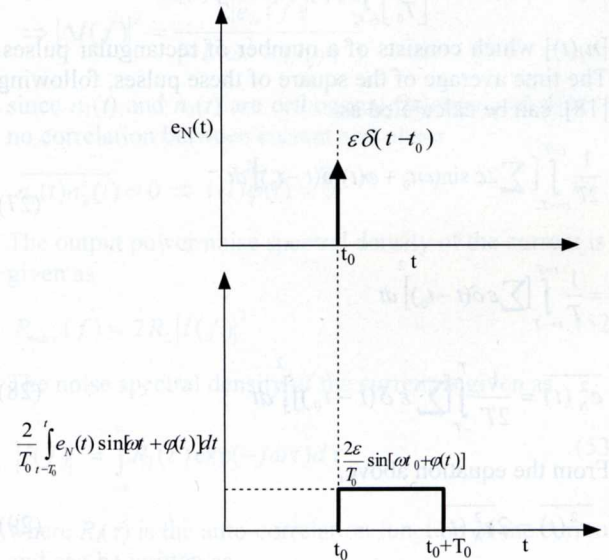


Figure 10 — The amplitude of the rectangular pulse.

The integral of the single noise pulse above gives the rectangular pulse with the height $\left[\frac{2}{T_0}\right] \varepsilon \sin[\omega t + \varphi(t)]$ and the length of T_0 as shown in Figure 10.

The integration of the single elementary noise pulse, following the Dirac Δ function, results in

$$\left[\frac{2}{T_0}\right] \int_{t-T_0}^t e_N(t) \sin[\omega t + \varphi(t)] dt \quad (25)$$

$$\approx \left[\frac{2}{T_0}\right] \int_{t-T_0}^t \varepsilon \delta(t-t_0) \sin[\omega t + \varphi(t)] dt$$

$$\left[\frac{2}{T_0}\right] \int_{t-T_0}^t \varepsilon \delta(t-t_0) \sin[\omega t + \varphi(t)] dt \quad (26)$$

$$\approx \left[\frac{2}{T_0}\right] \varepsilon \sin[\omega t_0 + \varphi(t)]$$

since the length of time T_0 is considered to be sufficiently small for any variation of $\varphi(t)$ and $I(t)$ during the time T_0 . The corresponding rectangular pulse of the magnitude $\frac{2}{T_0} \varepsilon \sin[\omega t_0 + \varphi(t)]$ is considered to be another pulse located at $t = t_0$ and can be expressed in the form of an impulse function with the amplitude $2\varepsilon \sin[\omega t_0 + \varphi(t)]$ located at $t = t_0$ for calculating the effect using Equations (21) and (22).

The effect of $\left[\frac{2}{T_0}\right] \int_{t-T_0}^t e_N(t) \sin[\omega t + \varphi(t)] dt$ is given by

$[n_1(t)]$ which consists of a number of rectangular pulses. The time average of the square of these pulses, following [18], can be calculated as

$$\frac{1}{2T} \int_{t=-T}^{t=T} \left[\sum 2\varepsilon \sin(\omega t_0 + \varphi(t)) \delta(t-t_0) \right]^2 dt \quad (27)$$

$$= \frac{1}{T} \int_{t=-T}^{t=T} \left[\sum \varepsilon \delta(t-t_0) \right]^2 dt$$

$$\overline{e_N^2(t)} = \frac{1}{2T} \int_{-T}^T \left[\sum \varepsilon \delta(t-t_0) \right]^2 dt \quad (28)$$

From the equation above,

$$\overline{n_1^2(t)} = 2\overline{e_N^2(t)} \quad (29)$$

Similarly, the total response of

$\frac{2}{T_0} \int_{t-T_0}^t e_N(t) \cos[\omega t + \varphi(t)] dt$ can be expressed by $[n_2(t)]$, which consists of a large number of such pulses and the time average of the square of these pulses is

$$\overline{n_2^2(t)} = 2\overline{e_N^2(t)} \quad (30)$$

since $\frac{2}{T_0} \int_{t-T_0}^t e_N(t) \sin[\omega t + \varphi(t)] dt$

and $\frac{2}{T_0} \int_{t-T_0}^t e_N(t) \cos[\omega t + \varphi(t)] dt$ are orthogonal functions,

and in the frequency domain are the upper and lower side bands relative to the carrier, and the correlation of $[n_1(t)]$ and $[n_2(t)]$ is

$$\overline{n_1(t)n_2(t)} = 0 \quad (31)$$

Now consider the narrow band noise signal, which is

$$e_N(t) = e_{N1}(t) + e_{N2}(t) \quad (32)$$

$$e_{N1}(t) = e_1(t) \sin[\omega_0 t + \varphi(t)] \quad (33)$$

$$e_{N2}(t) = -e_2(t) \cos[\omega_0 t + \varphi(t)] \quad (34)$$

where $e_{N1}(t)$ and $e_{N2}(t)$ are orthogonal functions, and $e_1(t)$ and $e_2(t)$ are slowly varying functions of time.

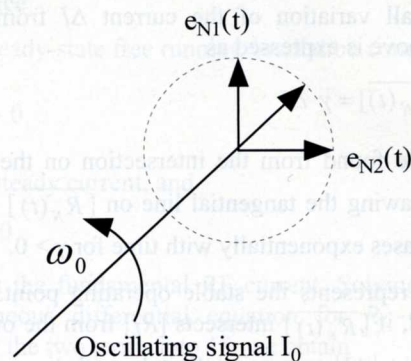


Figure 11 — Vector presentation of the oscillator signal and its modulation by the voltage e_{N1} and e_{N2} .

The calculation of $I_n(t)$ and $\varphi_n(t)$ for the free running oscillator can be derived from Equations (21) and (22) as

$$\left[\frac{2}{IT_0}\right] \int_{t-T_0}^t e_N(t) \sin[\omega t + \varphi(t)] dt \quad (35)$$

$$= -\frac{d\varphi(t)}{dt} \left[L + \frac{1}{\omega^2 C} \right] + \left[-\omega L + \frac{1}{\omega C} \right]$$

$$\left[\frac{2}{IT_0} \right] \int_{t-T_0}^t e_N(t) \sin[\omega t + \varphi(t)] dt \Rightarrow \left[\frac{1}{I} \right] n_1(t) \quad (36)$$

at resonance frequency $\omega = \omega_0$,

$$\left\{ -\frac{d\varphi(t)}{dt} \left[L + \frac{1}{\omega^2 C'} \right] + \left[-\omega L + \frac{1}{\omega C'} \right] \right\}_{\omega=\omega_0} \quad (37)$$

$$= -2L \frac{d\varphi(t)}{dt}$$

and

$$\frac{1}{I} n_1(t) = -2L \frac{d\varphi(t)}{dt} \quad (38)$$

$$\frac{d\varphi(t)}{dt} = -\left[\frac{1}{2LI} \right] n_1(t) \quad (39)$$

If Equation (39) is transformed in the frequency domain, $\varphi(f)$ can be expressed as

$$\varphi(f) = \frac{n_1(f)}{2\omega LI} \quad (40)$$

Now the spectral density of $[\varphi(f)]$ is

$$|\varphi(f)|^2 = \frac{1}{4\omega^2 L^2 I^2} |n_1(f)|^2 \quad (41)$$

$$\frac{1}{4\omega^2 L^2 I^2} |n_1(f)|^2 = \frac{2|e_N(f)|^2}{4\omega^2 L^2 I^2} \quad (42)$$

$$\Rightarrow |\varphi(f)|^2 = \frac{2|e_N(f)|^2}{4\omega^2 L^2 I^2}$$

where f varies from $-\infty$ to $+\infty$.

The amplitude of the current can be written as $I(t) = I_0 + \Delta I(t)$, where I_0 represents the stable operating point of the free-running oscillator with a loop gain slightly greater than 1.

From Equation (22), we can calculate

$$\begin{aligned} & \frac{2}{T_0} \int_{t-T_0}^t e_N(t) \cos[\omega t + \varphi(t)] dt \\ &= \frac{dI(t)}{dt} \left(L + \frac{1}{\omega^2 C'} \right) + [R_L - \overline{R_N(t)}] I(t), \end{aligned}$$

$$\left[\frac{2}{T_0} \int_{t-T_0}^t e_N(t) \cos[\omega t + \varphi(t)] dt \right]_{\omega=\omega_0} \quad (43)$$

$$= \left[2L \frac{\partial}{\partial t} [\Delta I(t)] + \Delta I(t) I_0 \gamma + \Delta I^2(t) \gamma \right]$$

Since the amplitude of $\Delta I^2(t)$ is negligible, its value can be set to 0;

$$\left[2L \frac{\partial}{\partial t} [\Delta I(t)] + \Delta I(t) I_0 \gamma + \Delta I^2(t) \gamma \right] \quad (44)$$

$$= 2L \frac{\partial}{\partial t} [\Delta I(t)] + \Delta I(t) I_0 \gamma$$

$$n_2(t) = \frac{2}{T_0} \int_{t-T_0}^t e_N(t) \cos[\omega t + \varphi(t)] dt \quad (45)$$

$$n_2(t) = 2L \frac{\partial}{\partial t} [\Delta I(t)] + \Delta I(t) I_0 \gamma \quad (46)$$

$$n_2(f) = 2L \omega \Delta I(f) + \Delta I(f) I_0 \gamma \quad (47)$$

The spectral density of $[n_2(f)]$ is

$$|n_2(f)|^2 = [4L^2 \omega^2 + (I_0 \gamma)^2] |\Delta I(f)|^2 \quad (48)$$

and the spectral density of $\Delta I(f)$ can be expressed in terms of $|n_2(f)|^2$ as

$$|\Delta I(f)|^2 = \frac{1}{[4L^2 \omega^2 + (I_0 \gamma)^2]} |n_2(f)|^2 \quad (49)$$

$$|n_2(f)|^2 = 2|e_N(f)|^2 \quad (50)$$

$$\Rightarrow |\Delta I(f)|^2 = \frac{2|e_N(f)|^2}{[4L^2 \omega^2 + (I_0 \gamma)^2]}$$

since $n_1(t)$ and $n_2(t)$ are orthogonal function and there is no correlation between current and phase

$$\overline{n_1(t)n_2(t)} = 0 \Rightarrow \overline{I(t)\varphi(t)} = 0 \quad (51)$$

The output power noise spectral density of the current is given as

$$P_{noise}(f) = 2R_L |I(f)|^2 \quad (52)$$

The noise spectral density of the current is given as

$$|I(f)|^2 = \int_{-\infty}^{\infty} R_I(\tau) \exp(-j\omega\tau) d\tau \quad (53)$$

where $R_I(\tau)$ is the auto-correlation function of the current and can be written as

$$R_I(\tau) = \overline{\left[\frac{I(t)I(t+\tau) \cos[\omega_0 t + \varphi(t)] \cos[\omega_0(t+\tau)]}{\varphi(t+\tau)} \right]} \quad (54)$$

$$R_I(\tau) = \frac{1}{2} \left[I_0^2 + R_{\Delta I}(\tau) \right] \overline{\cos(\omega_0 \tau) \cos(\varphi(t+\tau) - \varphi(t))} \quad (55)$$

Since $I(t)$ and $\varphi(t)$ are uncorrelated, auto-correlation function of the current $R_I(\tau)$ can be given as

From [18], but taking into consideration that both side bands are correlated, we can write

$$R_I(\tau) = \frac{1}{2} \left[I_0^2 + \frac{2|e_N(\tau)|^2}{2L\gamma I_0} \exp\left(-\frac{\gamma I_0}{2L} |\tau|\right) \right] \quad (56)$$

$$\exp\left(-\frac{|e_N(\tau)|^2}{4L^2 I_0^2} |\tau|\right) \cos(\omega_0 \tau)$$

Since the publication [18] skipped many stages of the calculation, up to here, a more complete and detailed flow is shown. These results are needed to calculate the noise performance at the component level later. Note the factor of 2, which results from the correlation.

Considering $\frac{\gamma I_0}{2L} \gg \frac{2|e_N(\tau)|^2}{4L^2 I_0^2}$, the noise spectral density of the current is given by

$$|I(f)|^2 = \int_{-\infty}^{\infty} R_I(\tau) \exp(-j\omega \tau) d\tau \quad (57)$$

with $I = I_0 + \Delta I(t)$; all RF-currents.

$$|I(f)|^2 = \frac{|e_N(f)|^2}{8L^2} \left[\frac{1}{(\omega - \omega_0)^2 + \left(\frac{|e_N(f)|^2}{4L^2 I_0^2}\right)^2} + \frac{1}{(\omega + \omega_0)^2 + \left(\frac{|e_N(f)|^2}{4L^2 I_0^2}\right)^2} \right] + \frac{|e_N(f)|^2}{8L^2} \left[\frac{1}{(\omega - \omega_0)^2 + \left(\frac{\gamma I_0}{2L}\right)^2} + \frac{1}{(\omega + \omega_0)^2 + \left(\frac{\gamma I_0}{2L}\right)^2} \right] \quad (58)$$

With

$$\left[\frac{1}{(\omega - \omega_0)^2 + \left(\frac{|e_N(f)|^2}{4L^2 I_0^2}\right)^2} + \frac{1}{(\omega + \omega_0)^2 + \left(\frac{|e_N(f)|^2}{4L^2 I_0^2}\right)^2} \right] \rightarrow \text{FM noise} \quad (59)$$

$$\left[\frac{1}{(\omega - \omega_0)^2 + \left(\frac{\gamma I_0}{2L}\right)^2} + \frac{1}{(\omega + \omega_0)^2 + \left(\frac{\gamma I_0}{2L}\right)^2} \right] \rightarrow \text{AM noise} \quad (60)$$

Since

$$\frac{\gamma I_0}{2L} \gg \frac{2|e_N(\tau)|^2}{4L^2 I_0^2}$$

for $\omega \rightarrow \omega_0$, FM noise predominates over the AM noise.

For $\omega \gg \omega_0$, both the FM noise and AM noise terms give equal contribution.

Considering $\omega + \omega_0 \gg \omega - \omega_0$, then

$$|I(f)|^2 = \frac{|e_N(f)|^2}{8L^2} \left[\frac{1}{(\omega - \omega_0)^2 + \left(\frac{|e_N(f)|^2}{4L^2 I_0^2}\right)^2} + \frac{1}{(\omega - \omega_0)^2 + \left(\frac{\gamma I_0}{2L}\right)^2} \right] \quad (61)$$

$$P_{\text{noise}}(f) = 2R_L |I(f)|^2 \quad (62)$$

$$P_{\text{noise}}(f) = 2R_L \left(\frac{|e_N(f)|^2}{8L^2} \right) \left[\frac{1}{(\omega - \omega_0)^2 + \left(\frac{|e_N(f)|^2}{4L^2 I_0^2}\right)^2} + \frac{1}{(\omega - \omega_0)^2 + \left(\frac{\gamma I_0}{2L}\right)^2} \right] \quad (63)$$

Since $R_{\text{Load}} = R_L + R_o$, the effective dynamic resistance of the free running oscillator is given by

$$\sum_{\text{effective}} |R_{\text{tot}}| = R_N(t) - R_{\text{Load}} = R_o \quad (64)$$

where R_o is the output resistance; $R_o - R_{\text{tot}} = 0$.

The Q of the resonator circuit is expressed as

$$Q_L = \frac{\omega L}{R_0} \quad (65)$$

The oscillator output noise power in terms of Q is given by

$$P_{noise}(f) = \frac{\omega_0^2 |e|^2}{2Q_L^2 2R_N(t)} \left[\frac{1}{(\omega - \omega_0)^2 + \left(\frac{\omega_0^2}{4Q_L^2}\right)^2 \left(\frac{|e|^2}{2R_N(t)P_{out}}\right)^2} + \frac{1}{(\omega - \omega_0)^2 + \left(\frac{\omega_0^2}{Q_L^2}\right)^2 \left(\frac{\gamma I_0}{2R_N(t)}\right)^2} \right] \quad (66)$$

Figure 12 shows the Colpitts oscillator with a series resonator and the small signal ac equivalent circuit.

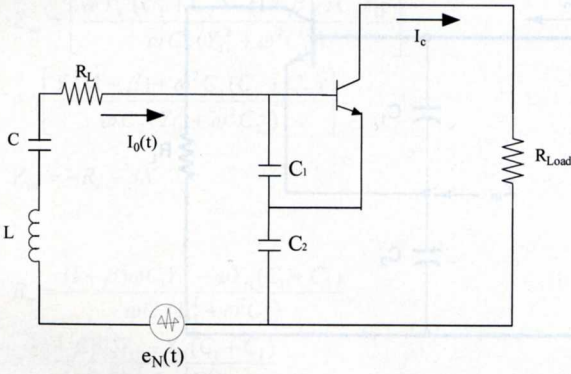


Figure 12 — Colpitts oscillator with series resonator and small signal ac equivalent circuit.

From the analytical expression of the noise analysis above, the influence of the circuit components on the phase noise can be explicitly calculated as

$$|\varphi(f)|^2 = \frac{1}{4\omega^2 L^2 I_0^2(f)} |n_1(f)|^2 \quad (67)$$

$$\frac{1}{4\omega^2 L^2 I_0^2(f)} |n_1(f)|^2 = \frac{2|e_N(f)|^2}{4\omega^2 L^2 I_0^2(f)} \quad (68)$$

$$\Rightarrow |\varphi(f)|^2 = \frac{2|e_N(f)|^2}{4\omega^2 L^2 I_0^2(f)}$$

where the frequency f varies from $-\infty$ to $+\infty$.

The resulting single sideband phase noise is

$$\mathfrak{F} = \frac{|e_N(f)|^2}{4\omega^2 L^2 I_0^2(f)} \quad (69)$$

The unknown variables are $|e_N(f)|^2$ and $I_0^2(f)$, which need to be determined next. $I_0^2(f)$ will be transformed into $I_{c0}^2(f)$ by multiplying $I_0^2(f)$ with the effective current gain $Y_{21}^+/Y_{11}^+ = \beta^*$.

Calculation of $I_{c0}^2(f)$

From Figure 12, the LC-series resonant circuit is in shunt between the base and the emitter with the capacitive negative conductance portion of the transistor. We now introduce a collector load R_{Load} at the output, or better yet, an impedance Z .

The oscillator base current $i(t)$ is

$$i(t) = |I_0| \cos(\omega t) = \frac{V_{bc}(t)}{Z} \quad (70)$$

and the collector current is

$$|I_{c0}| = \left| \frac{[0.7 - V_{ce}]}{R_{Load} + j\left(\omega L - \frac{1}{\omega C_{IN}}\right)} \right| \quad (71)$$

$$\approx \left| \frac{V_{ce}}{R_{Load} + j\left(\omega L - \frac{1}{\omega C_{IN}}\right)} \right|$$

$$\overline{I_{c0}^2(f)} \approx \left\{ \frac{\overline{V_{ce}^2(f)}}{[R_{Load}]^2 + \left(\omega L - \frac{1}{\omega C_{IN}}\right)^2} \right\} \quad (72)$$

$$= \left\{ \frac{\overline{V_{ce}^2(f)}}{\left[\frac{\omega L}{Q}\right]^2 + \left(\omega L - \frac{1}{\omega C_{IN}}\right)^2} \right\}$$

The voltage V_{ce} is the RF voltage across the collector-emitter terminals of the transistor. Considering the steady-state oscillation $\omega \rightarrow \omega_0$, the total loss resistance is compensated by the negative resistance of the active device as $R_L = \overline{R_N(t)}$. The expression of $\left|I_{c0}^2(f)\right|_{\omega=\omega_0}$ is

$$\left|I_{c0}^2(f)\right|_{\omega=\omega_0} = \left| \frac{\overline{V_{ce}^2(f)}}{\left[\frac{\omega_0 L}{Q}\right]^2 + \left(\omega_0 L - \frac{1}{\omega_0 C_{IN}}\right)^2} \right| \quad (73)$$

$$= \left| \frac{\overline{V_{ce}^2(f)}}{(\omega_0 L)^2 \left[\frac{1}{Q^2} + \left(1 - \frac{1}{\omega_0^2 LC_{IN}}\right)^2 \right]} \right|$$

$$\overline{I_{c0}^2(f)}_{\omega=\omega_0} = \frac{\overline{V_{ce}^2(f)}}{(\omega_0 L)^2 \left[\frac{1}{Q^2} + \left(1 - \frac{1}{\omega_0^2 L} \frac{C_1 + C_2}{C_1 C_2} \right)^2 \right]} \quad (74)$$

where C_{IN} is the equivalent capacitance of the negative resistor portion of the oscillator circuit.

$$C' = \frac{CC_{IN}}{C + C_{IN}}, \quad C_{IN} = \frac{C_1 C_2}{C_1 + C_2} \quad (75)$$

$$Q = \frac{\omega L}{R_L} \quad (76)$$

For a reasonably high Q resonator $\overline{I_{c0}^2(f)}_{\omega=\omega_0} \propto [C_{IN}]_{\omega=\omega_0}$

Calculation of the noise voltage $e_N(f)$

The equivalent noise voltage from the negative resistance portion of the oscillator circuit is given an open-circuit noise voltage [EMF] of the circuit as shown in Figure 13 below.

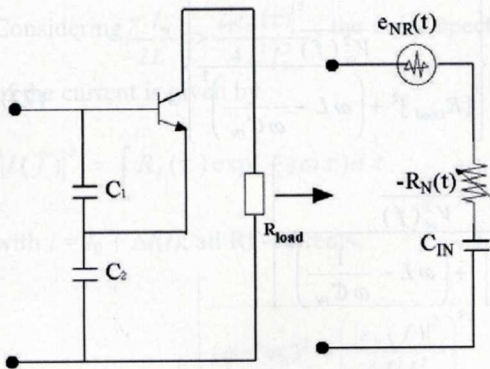


Figure 13 — Equivalent representation of negative resistance portion of the circuit at the input for the open circuit noise voltage.

The noise voltage associated with the resonator loss resistance R_s is

$$\overline{e_R^2(f)}_{\omega=\omega_0} = 4kTBR_s \quad (77)$$

R_s denotes the equivalent series loss resistor, which can be calculated from the parallel loading resistor R_{load} , see Figure 12.

$$\overline{e_R^2(f)}_{\omega=\omega_0} = 4kTR \text{ for } B = 1 \text{ Hz bandwidth} \quad (78)$$

The total noise voltage power within 1 Hz bandwidth can be given as

$$\overline{e_N^2(f)}_{\omega=\omega_0} = \overline{e_R^2(f)} + \overline{e_{NR}^2(f)} \quad (79)$$

Derivation of Equation (80):

The total noise voltage power within 1 Hz bandwidth can be given as

$$\overline{e_N^2(f)}_{\omega=\omega_0} = \overline{e_R^2(f)} + \overline{e_{NR}^2(f)} \quad (80)$$

The first term in Equation (80) is the noise voltage power due to the loss resistance R , and the second term is associated with the negative resistance of the active device R_N .

Figure 14 and 15 illustrate the oscillator circuit for the purpose of the calculation of the negative resistance.

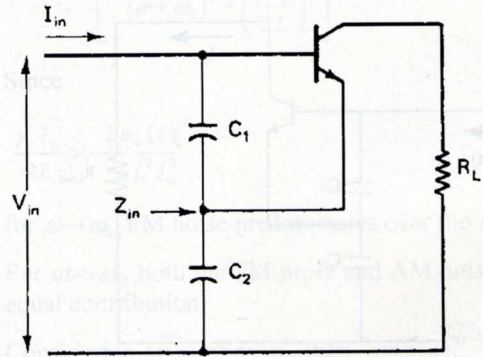


Figure 14 — Oscillator circuit for the calculation of the negative resistance.

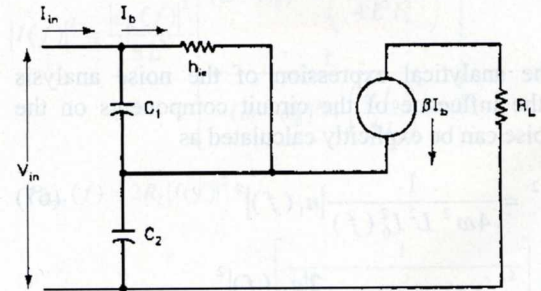


Figure 15 — Equivalent oscillator circuit for the calculation of the negative resistance.

From Figure 15, the circuit equation is given from Kirchoff's voltage law (KVL) as

$$V_{in} = I_{in}(X_{C_1} + X_{C_2}) - I_b(X_{C_1} - \beta X_{C_2}) \quad (81)$$

$$0 = -I_{in}(X_{C_1}) + I_b(X_{C_1} + h_{ie}) \quad (82)$$

Considering, $\frac{1}{Y_{11}} = h_{ie}$

$$Z_{in} = \frac{V_{in}}{I_{in}} = \frac{(1 + \beta)X_{C_1}X_{C_2} + h_{ie}(X_{C_1} + X_{C_2})}{X_{C_1} + h_{ie}} \quad (83)$$

$$Z_{in} = \frac{\left(-\frac{(1+\beta)}{\omega^2 C_1 C_2} + \frac{(C_1 + C_2)}{j\omega C_1 C_2} \frac{1}{Y_{11}} \right)}{\left(\frac{1}{Y_{11}} + \frac{1}{j\omega C_1} \right)} \quad (84)$$

$$Z_{in} = \frac{-jY_{11}(1+\beta) + \omega(C_1 + C_2)}{\omega C_2(Y_{11} + j\omega C_1)} \quad (85)$$

$$Z_{in} = \frac{[\omega(C_1 + C_2) - jY_{11}(1+\beta)][Y_{11} - j\omega C_1]}{\omega C_2(Y_{11}^2 + \omega^2 C_1^2)} \quad (86)$$

$$Z_{in} = \left[\frac{\omega Y_{11}(C_1 + C_2) - (1+\beta)\omega C_1 Y_{11}}{\omega C_2(Y_{11}^2 + \omega^2 C_1^2)} \right] - j \left[\frac{Y_{11}^2(1+\beta) + \omega^2 C_1(C_1 + C_2)}{\omega C_2(Y_{11}^2 + \omega^2 C_1^2)} \right] \quad (87)$$

$$Z_{in} = -R_n - jX \quad (88)$$

$$R_n = \frac{(1+\beta)\omega C_1 Y_{11} - \omega Y_{11}(C_1 + C_2)}{\omega C_2(Y_{11}^2 + \omega^2 C_1^2)} \quad (89)$$

$$= \frac{(1+\beta)C_1 Y_{11} - Y_{11}(C_1 + C_2)}{C_2(Y_{11}^2 + \omega^2 C_1^2)}$$

$$R_n = \frac{\beta C_1 Y_{11} - Y_{11} C_2}{C_2(Y_{11}^2 + \omega^2 C_1^2)} \quad (90)$$

$$= \frac{\beta Y_{11}}{C_2(Y_{11}^2 + \omega^2 C_1^2)} - \frac{Y_{11}}{(Y_{11}^2 + \omega^2 C_1^2)}$$

Considering $\beta = \frac{Y_{21}}{Y_{11}} \approx \frac{g_m}{Y_{11}}$

$$R_n = \frac{g_m}{C_2(\frac{g_m^2}{\beta^2} + \omega^2 C_1^2)} - \frac{g_m/\beta}{(\frac{g_m^2}{\beta^2} + \omega^2 C_1^2)} \quad (91)$$

$$R_n = \frac{g_m \beta^2 C_1}{(g_m^2 C_2 + \omega^2 \beta^2 C_1^2 C_2)} - \frac{g_m \beta}{(g_m^2 + \beta^2 \omega^2 C_1^2)} \quad (92)$$

$$R_n = \frac{g_m \beta^2 \omega^2 C_1 C_2}{\omega^2 C_1^2 (\frac{C_2^2}{C_1^2} g_m^2 + \omega^2 \beta^2 C_2^2)} - \frac{g_m \beta \omega^2 C_2^2}{\omega^2 C_1^2 (\frac{C_2^2}{C_1^2} g_m^2 + \beta^2 \omega^2 C_2^2)} \quad (93)$$

$$R_n = \left[\frac{g_m^2}{\omega^2 C_1^2 (\frac{C_2^2}{C_1^2} g_m^2 + \omega^2 \beta^2 C_2^2)} \right] \left[\frac{\beta^2 \omega^2 C_1 C_2}{g_m} - \frac{\beta \omega^2 C_2^2}{g_m} \right] \quad (94)$$

$$R_n = \left[\frac{g_m^2}{\omega^2 C_1^2 (\frac{C_2^2}{C_1^2} g_m^2 + \omega^2 \beta^2 C_2^2)} \right] \left[g_m \left[\left(\frac{\omega C_1}{Y_{11}} \right) \left(\frac{\omega C_2}{Y_{11}} \right) - \frac{\omega^2 C_2^2}{\beta Y_{11}^2} \right] \right] \quad (95)$$

$$R_n = \left[\frac{g_m^2}{\omega^2 C_1^2 (\frac{C_2^2}{C_1^2} g_m^2 + \omega^2 \beta^2 C_2^2)} \right] \left[g_m \left[\left(\frac{\omega C_1}{Y_{11}} \right) \left(\frac{\omega C_2}{Y_{11}} \right) - \frac{1}{\beta} \left(\frac{\omega C_2}{Y_{11}} \right) \left(\frac{\omega C_2}{Y_{11}} \right) \right] \right] \quad (96)$$

Considering $\left(\frac{\omega C_1}{Y_{11}} \right) \left(\frac{\omega C_2}{Y_{11}} \right) \gg \frac{1}{\beta} \left(\frac{\omega C_2}{Y_{11}} \right) \left(\frac{\omega C_2}{Y_{11}} \right)$

and $\left(\frac{\omega C_1}{Y_{11}} \right) \left(\frac{\omega C_2}{Y_{11}} \right) \approx 1$ (97)

$$\left[g_m \left[\left(\frac{\omega C_1}{Y_{11}} \right) \left(\frac{\omega C_2}{Y_{11}} \right) - \frac{1}{\beta} \left(\frac{\omega C_2}{Y_{11}} \right) \left(\frac{\omega C_2}{Y_{11}} \right) \right] \right] \quad (98)$$

$$\cong \frac{I_c}{V_T} = \frac{I_c}{kT/q} \Rightarrow \frac{qI_c}{kT}$$

From (96) and (98)

$$R_n = \left[\frac{g_m^2}{\omega^2 C_1^2 (\frac{C_2^2}{C_1^2} g_m^2 + \omega^2 \beta^2 C_2^2)} \right] \frac{qI_c}{kT} \quad (99)$$

From (80), the total noise voltage power within a 1 Hz bandwidth can be given as

$$\overline{e_N^2(f)}_{\omega=\omega_0} = \overline{e_R^2(f)} + \overline{e_{NR}^2(f)} \quad (100)$$

$$\overline{e_N^2(f)}_{\omega=\omega_0} = [4kTR] + \left[\frac{4qI_c g_m^2 + \frac{K_f I_b^{AF}}{\Delta\omega} g_m^2}{\omega_0^2 C_1^2 (\omega_0^2 (\beta^+)^2 C_2^2 + g_m^2 \frac{C_2^2}{C_1^2})} \right] \quad (101)$$

where

$$\beta^+ = \left[\frac{Y_{21}}{Y_{11}} \right] \left[\frac{C_1}{C_2} \right]^p, \quad g_m = [Y_{21}^+] \left[\frac{C_1}{C_2} \right]^q, \text{ redefined}$$

$$\overline{e_N^2(f)}_{\omega=\omega_0} = [4kTR] + \left[\frac{4qI_{c0}g_m^2 + \frac{K_f I_b^{AF}}{\Delta\omega} g_m^2}{\omega_0^2 C_1^2 (\omega_0^2 (\beta^+)^2 C_2^2 + g_m^2 \frac{C_2^2}{C_1^2})} \right] \quad (102)$$

where

$$\beta^+ = \left[\frac{Y_{21}^+}{Y_{11}^+} \right] \left[\frac{C_1}{C_2} \right]^p, \quad g_m = \left[Y_{21}^+ \right] \left[\frac{C_1}{C_2} \right]^q, \quad \text{redefined.}$$

The values of p and q depend upon the drive level.

The flicker noise contribution in Equation (80) is introduced by adding term $\frac{K_f I_b^{AF}}{\Delta\omega}$ in I_{c0} , where K_f is the flicker noise coefficient and AF is the flicker noise exponent. This is valid only for the bipolar transistor. For an FET, the equivalent currents have to be used.

In this case we use a value of 10^{-8} , some publications claim much smaller numbers such as 10^{-11} . The authors must have done some magic to get the measured curve fitted. In my opinion these small numbers violate the laws of physics for bipolar transistors.

The first term in the expression above is related to the thermal noise due to the loss resistance of the resonator tank and the second term is related to the shot noise and flicker noise in the transistor.

Now, the phase noise of the oscillator can be expressed as

$$\overline{\varphi^2(\omega)} = \frac{2\overline{e_N^2(\omega)}}{4\omega_0^2 L^2 I_0^2(\omega)} \quad (103)$$

$$\overline{\varphi^2(\omega)}_{SSB} = \frac{1}{2} \overline{\varphi^2(\omega)} = \frac{\overline{e_N^2(\omega)}}{4\omega_0^2 L^2 I_0^2(\omega)} \quad (104)$$

$$\overline{\varphi^2(\omega)}_{SSB} = \left[4kTR + \frac{4qI_{c0}g_m^2 + \frac{K_f I_b^{AF}}{\omega} g_m^2}{\omega_0^2 C_1^2 (\omega_0^2 (\beta^+)^2 C_2^2 + g_m^2 \frac{C_2^2}{C_1^2})} \right] \quad (105)$$

$$\left[\frac{(\omega_0)^2 \left[\frac{1}{Q^2} + \left(1 - \frac{1}{\omega_0^2 L} \frac{C_1 + C_2}{C_1 C_2} \right)^2 \right]}{4\omega^2 |V_{ce}^2(\omega)|} \right]$$

$$\overline{\varphi^2(\omega)}_{SSB} = \left[4kTR + \frac{4qI_{c0}g_m^2 + \frac{K_f I_b^{AF}}{\omega} g_m^2}{\omega_0^2 C_1^2 (\omega_0^2 (\beta^+)^2 C_2^2 + g_m^2 \frac{C_2^2}{C_1^2})} \right] \quad (104)$$

$$\left[\frac{\omega_0^2}{4\omega^2 V_{ce}^2} \right] \left[\frac{1}{Q^2} + \left(1 - \frac{1}{\omega_0^2 L} \frac{C_1 + C_2}{C_1 C_2} \right)^2 \right]$$

Considering

$$\left(\frac{1}{\omega_0^2 L} \frac{C_1 + C_2}{C_1 C_2} \right) \gg 1; \text{ for}$$

$$\omega_0 = 2\pi f = 6.28 \times 10^9 \text{ Hz}, L = 10^{-9} \text{ H}, C_1 = 10^{-12} \text{ F}, C_2 = 10^{-12} \text{ F}$$

$$\left(\frac{1}{\omega_0^2 L} \frac{C_1 + C_2}{C_1 C_2} \right) = 50.7$$

Since the phase noise is always expressed in dBc/Hz, we now calculate, after simplification of Equation (84),

$$\xi(\omega) = 10 \log \left\{ \frac{4kTR + \frac{4qI_{c0}g_m^2 + \frac{K_f I_b^{AF}}{\omega} g_m^2}{\omega_0^2 C_1^2 (\omega_0^2 (\beta^+)^2 C_2^2 + g_m^2 \frac{C_2^2}{C_1^2})}}{\left[\frac{\omega_0^2}{4\omega^2 V_{ce}^2} \right] \left[\frac{1}{Q^2} + \frac{[C_1 + C_2]^2}{C_1^2 C_2^2 \omega_0^4 L^2} \right]} \right\} \quad (107)$$

For the bias condition (which is determined from the output power requirement), the loaded quality factor, and the device parameters [transconductance and β^+], the best phase noise can be found by differentiating $\overline{\varphi^2(\omega)}_{SSB}$ with respect to C_1/C_2 .

Considering that all the parameters of $\overline{\varphi^2(\omega)}_{SSB}$ are constants for a given operating condition (except the feedback capacitor), the minimum value of the phase noise can be determined for any fixed value of C_1 as

$$\overline{\varphi^2(\omega)} = \left[k_0 + \frac{k_1}{k_2 C_1^2 C_2^2 + k_3 C_2^2} \right] \left[\frac{C_1 + C_2}{C_1 C_2} \right]^2 \quad (108)$$

$$k_0 = \frac{kTR}{\omega^2 \omega_0^2 L^2 V_{ce}^2} \quad (109)$$

$$k_1 = \frac{qI_{c0}g_m^2 + \frac{K_f I_b^{AF}}{\omega} g_m^2}{\omega^2 \omega_0^2 L^2 V_{ce}^2} \quad (110)$$

$$k_2 = \omega_0^4 (\beta^+)^2 \quad (111)$$

$$k_3 = g_m^2 \quad (112)$$

Where k_1 , k_2 , and k_3 , are constant only for a particular drive level, with $y = C_1/C_2$. Making k_2 and k_3 also dependent on y , as the drive level changes, the final noise equation is

$$\mathfrak{L}(\omega) = 10 \times \log \left[\left[k_0 + \frac{k^3 k_1 \left[\frac{Y_{21}^+}{Y_{11}^+} \right]^2 [y]^{2p}}{[Y_{21}^+]^3 [y]^{3q}} \right] \left[\frac{[1+y]^2}{y^2} \right] \right] \quad (113)$$

$$\left[\frac{1}{(y^2 + k)} \right]$$

where

$$k_0 = \frac{kTR}{\omega^2 \omega_0^2 L^2 V_{cc}^2}$$

$$k_1 = \frac{qI_c g_m^2 + \frac{K_f I_b^{AF}}{\omega} g_m^2}{\omega^2 \omega_0^4 L^2 V_{cc}^2}$$

$$k_2 = \omega_0^2 (\beta^+)^2$$

Figure 16 shows the simulated phase noise and its minimum for two values of C_1 , 2 pF and 5 pF. 5 pF, provides a better phase noise and a flatter response. For larger C_1 , the oscillator will cease to oscillate.

$$\frac{\partial \phi^2(\omega, y, k)}{\partial y} \Rightarrow 0$$

$$\frac{\partial}{\partial y} \left\{ \left[k_0 + \frac{k^3 k_1 \left[\frac{Y_{21}^+}{Y_{11}^+} \right]^2 [y]^{2p}}{[Y_{21}^+]^3 [y]^{3q}} \right] \left[\frac{1}{(y^2 + k)} \right] \right\} \Rightarrow 0 \quad (114)$$

$$\left[\frac{[1+y]^2}{y^2} \right]_{y=m}$$

From curve-fitting attempts, the following values for q and p in Equation (114) were determined:

$$q=1 \text{ to } 1.1; p = 1.3 \text{ to } 1.6.$$

q and p are a function of the normalized drive level x and need to be determined experimentally.

The transformation factor n is defined as

$$n = 1 + \frac{C_1}{C_2} \rightarrow 1 + y \quad (115)$$

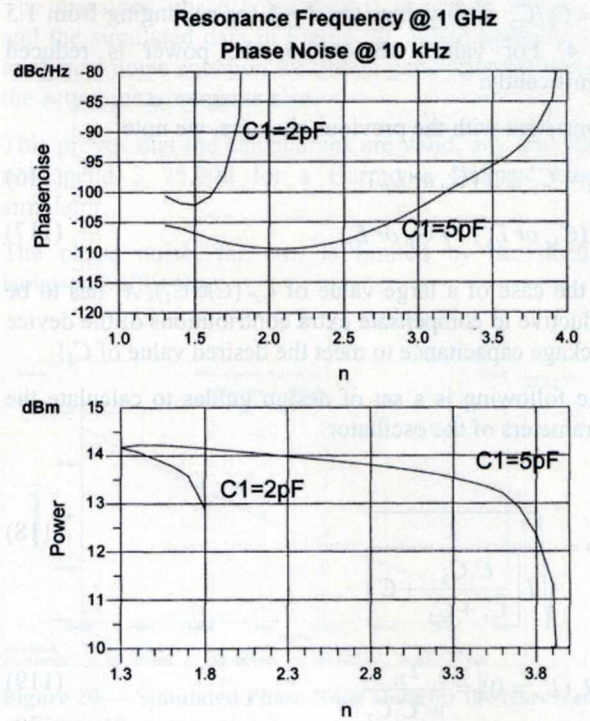


Figure 16 — Phase noise vs. n and output power.

The following plot in Figure 17 shows the predicted phase noise resulting from Equation (114). For the first time, the flicker corner frequency was properly implemented and gives answers consistent with the measurements. In the following chapter all the noise sources will be added, but the key contributors are still the resonator noise and the flicker noise. The Schottky noise dominates further out. The break point for the flicker noise can be clearly seen.

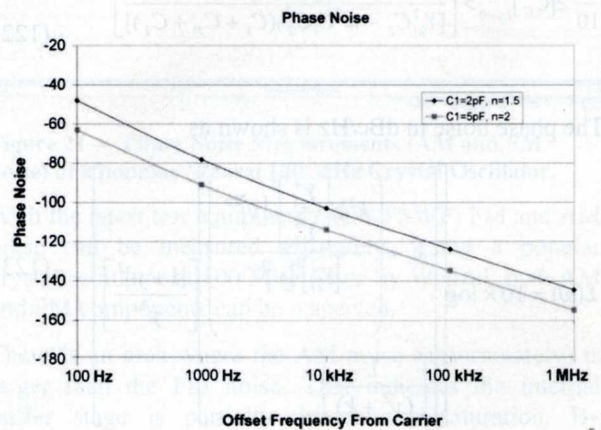


Figure 17 — Using Equation (114), the phase noise for different values of n for constant C_2 can be calculated.

Summary Results

The analysis of the oscillator in the time domain has given us a design criteria to find the optimum value of

$y = C_1/C_2$ with values for $y + 1$ (or n) ranging from 1.5 to 4. For values above 3.5, the power is reduced significantly.

Consistent with the previous chapters, we note

$$C_1 = C_1^* \pm X(C_P \text{ or } L_P) \quad (116)$$

$$X(C_{be} \text{ or } L_b) \rightarrow C_P \text{ or } L_P \quad (117)$$

In the case of a large value of C_P ($C_P > C_1$), X_1 has to be inductive to compensate extra contributions of the device package capacitance to meet the desired value of C_1 !

The following is a set of design guides to calculate the parameters of the oscillator.

$$\omega = \sqrt{\frac{1}{L \left[\frac{C_1 C_2}{C_1 + C_2} + C \right]}} \quad (118)$$

$$|R_n(L_P = 0)| = \frac{Y_{21}}{\omega^2 C_1 C_2} \quad (119)$$

$$C_1 = \frac{1}{\omega_0} \sqrt{\frac{Y_{11}}{K}} \quad (120)$$

C_2 is best determined graphically from the noise plot.

$$C_C > \left\{ \frac{(w^2 C_1 C_2)(1 + w^2 Y_{21}^2 L_P^2)}{[Y_{21}^2 C_2 - w^2 C_1 C_2](1 + w^2 Y_{21}^2 L_P^2)(C_1 + C_P + C_2)} \right\} \quad (121)$$

$$\frac{C}{10} \geq [C_C]_{L_P=0} > \left[\frac{(w^2 C_1 C_2)}{[Y_{21}^2 C_2 - w^2 C_1 C_2](C_1 + C_P + C_2)} \right] \quad (122)$$

The phase noise in dBc/Hz is shown as

$$\mathfrak{L}(\omega) = 10 \times \log \left[\left[k_0 + \frac{k^3 k_1 \left[\frac{Y_{21}^+}{Y_{11}^+} \right]^2 [y]^{2p}}{[Y_{21}^+]^q [y]^{3q}} \right] \left[\frac{[1+y]^2}{y^2} \right] \right] \left[\frac{1}{(y^2 + k)} \right] \quad (123)$$

The phase noise improves with the square of the loaded Q_L ! 10% higher $Q \rightarrow 20\%$ better phase noise!

$$L(\omega) \propto \frac{1}{C_{IN}^2} \quad (124)$$

The loaded Q of the resonator determines the minimum possible level of the oscillator phase noise for given bias voltage and oscillator frequency.

To achieve close to this minimum phase noise level set by the loaded Q_L of the resonator, the optimum (rather, how large the value of the C_{IN} can be) value of C_{IN} is to be fixed.

To achieve the best possible phase noise level, the feedback capacitors C_1 and C_2 should be made as large as possible, but still generate sufficient negative resistance for sustaining steady-state oscillation.

$$[-R_N]_{\text{negative resistance}} \propto \frac{1}{\omega_0^2} \frac{1}{C_1 C_2}, \text{ (no parasitics)} \quad (125)$$

The negative resistance of the oscillator circuit is inversely proportional to the feedback capacitors. Therefore, the limit of the feedback capacitor value is determined by the minimum negative resistance for a loop gain greater than unity.

From the phase noise equation discussed, the feedback capacitor C_2 has more influence compared to C_1 . The drive level and conduction angle of the Colpitts oscillator circuit is a strong function of C_2 .

The time domain approach has provided us with the design guide for the key components of the oscillator; however, it did not include all the noise sources of the transistor. By using the starting parameters, such as C_1 and C_2 and the bias point, as well as the information about the resonator and the transistor, a complete noise model/analysis will now be shown.

The time domain approach has provided us with the design guide for the key components of the oscillator; however, it did not include all the noise sources of the transistor. By using the starting parameters, such as C_1 and C_2 and the bias point, as well as the information about the resonator and the transistor, a complete noise model/analysis will be shown now.

After some lengthy calculations and approximations, adding shot noise, flicker noise and the loss resistor, the equivalent expression of the phase noise can be derived as

$$\mathfrak{L}(\omega) = \left[\frac{|g_m^2(t)(4qI_c) + |g_m^2(t) \left(\frac{K_f J_b^{AF}}{\omega} \right)|}{\omega_0^4 \beta^2 C_{ce}^2 (C_2 + C_{b'e} - L_1 C_2 C_{b'e} \omega_0^2)^2 + |g_m^2(t) \omega_0^2 (C_2 + C_{b'e} - L_1 C_2 C_{b'e} \omega_0^2)^2} \right] \times \left[\frac{\omega_0^2}{4\omega^2 V_{ce}^2} \left[\frac{Q^2}{Q_L^2} + \left(1 - \frac{1}{\omega_0^2 L_1} \left(\frac{[(C_2 + C_{b'e} - L_1 C_2 C_{b'e} \omega_0^2) + C_{ce}]}{C_{ce} [(C_2 + C_{b'e} - L_1 C_2 C_{b'e} \omega_0^2)]} \right) \right)^2 \right] \right] \quad (126)$$

The flicker noise contribution in equation (126) is introduced by adding term $K_f I_b^{AF} / \omega$ in RF collector current I_C , where K_f is the flicker noise coefficient and AF is the flicker noise exponent. This is valid only for the bipolar transistor. For an FET, the equivalent current transformations have to be used.

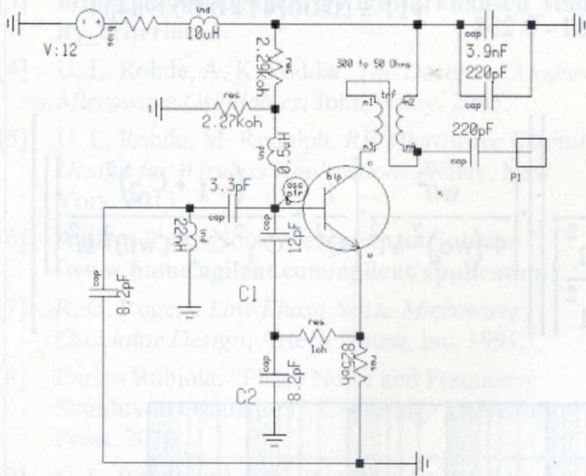


Figure 18 — Colpitts Configuration – Test Circuit.

This is the most complete noise model derived and tested.

Validation

After so many calculations a proof of concept is called for [14-20]. Figure 18 shows the test circuit. It is the typical Colpitts oscillator with the RF output taken from the collector. The transistor BFG 520 is made by Philips and is a 9 GHz NPN device used at a small fraction of I_C max.

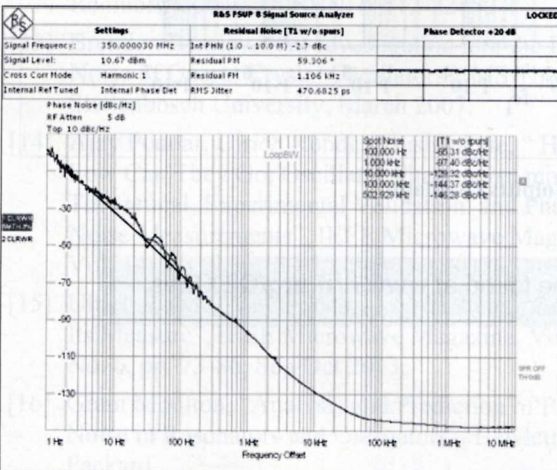


Figure 19: Measured Data for a 350MHz Oscillator.

The measured phase noise data is shown in Figure 19 and the simulated data in Figure 20. When applying the analytical noise equation we obtain good agreement with the actual measurements also.

This proves that the calculations are valid, any one need not spend \$ 25,000 for a Harmonic Balance based simulator.

The phase noise, far out, is limited by the needed isolation/buffer stage.

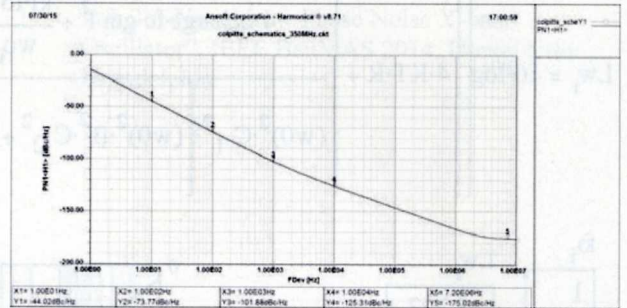


Figure 20 — Simulated Phase Noise Data for the test circuit of Figure 18.

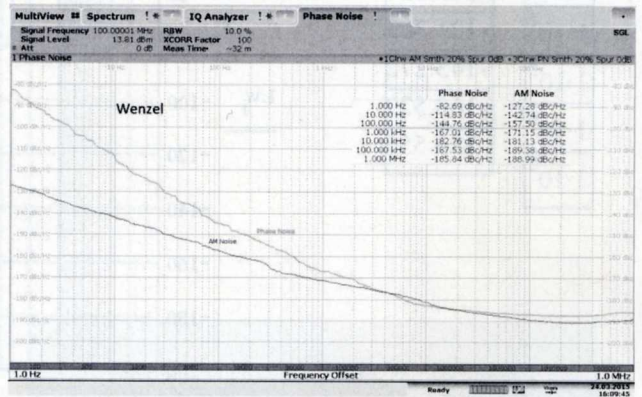


Figure 21 — Phase Noise Measurements (AM and FM noise) of a popular Wenzel 100 MHz Crystal Oscillator.

With the latest test equipment (R&S FSWP) FM and AM noise can be measured separately. Using a popular crystal oscillator at 100 MHz made by Wenzel, both AM and FM components can be inspected.

There is an area where the AM noise (unfortunately) is larger than the FM noise. That indicates the internal buffer stage is partially driven into saturation. By changing some component values this can be avoided.

$$I_c = 6.2 \cdot 10^{-3} \quad I_b = 43.2 \cdot 10^{-6} \quad L = 22 \cdot 10^{-9} \quad C_1 = 12 \cdot 10^{-12} \quad C_2 = 8.2 \cdot 10^{-12} \quad C_c = 3.3 \cdot 10^{-12}$$

$$q_{charge} = 1.602 \cdot 10^{-19} \quad T = 300 \text{ K} = 1.3806 \cdot 10^{-23} \text{ R} = 0.3 \quad k_f = 1 \cdot 10^{-7} \quad af = 2 \quad KT = 4.143 \cdot 10^{-21}$$

$$Q_{mac} = 120 \quad Q = 60 \quad V_t = 12 \quad f = 350 \cdot 10^6 \quad \omega_0 = 2 \pi \cdot f \quad \beta = 140 \quad y_{21} = (0.193 - 0.0051j)$$

$$i = 0..7 \quad f_{i1} = 10^i \quad r_e = \frac{26 \cdot 10^{-3}}{I_c} \quad gm_1 = \frac{1}{r_e} \quad gm_1 = 0.238 \quad y_{11} = (0.00141 + 0.000984j)$$

$$\omega_{o1} = 2 \cdot \pi \cdot f_{i1}$$

$$Lw_i = 10 \cdot \log \left[4 \cdot KT \cdot R + \frac{4 \cdot q_{charge} \cdot I_c \cdot gm_1^2 + \frac{k_f \cdot I_b^{af} \cdot gm_1^2}{\omega_{o1}}}{(\omega_0^2 \cdot C_1^2 \cdot (\omega_0^2 \cdot \beta^2 \cdot C_2^2 + gm_1^2 \cdot \frac{C_2^2}{C_1^2}))} \cdot \left[\frac{\omega_0^2}{4 \cdot (\omega_{o1})^2 \cdot V_t^2} \cdot \left[\frac{1}{Q^2} + \frac{(C_1 + C_2)^2}{C_1^2 \cdot C_2^2 \cdot (\omega_0)^4 \cdot L^2} \right] \right] \right]$$

f_{i1}	Lw_i
1	-5.227
10	-35.222
100	-65.165
$1 \cdot 10^3$	-94.633
$1 \cdot 10^4$	-121.303
$1 \cdot 10^5$	-143.272
$1 \cdot 10^6$	-163.529
$1 \cdot 10^7$	-183.555

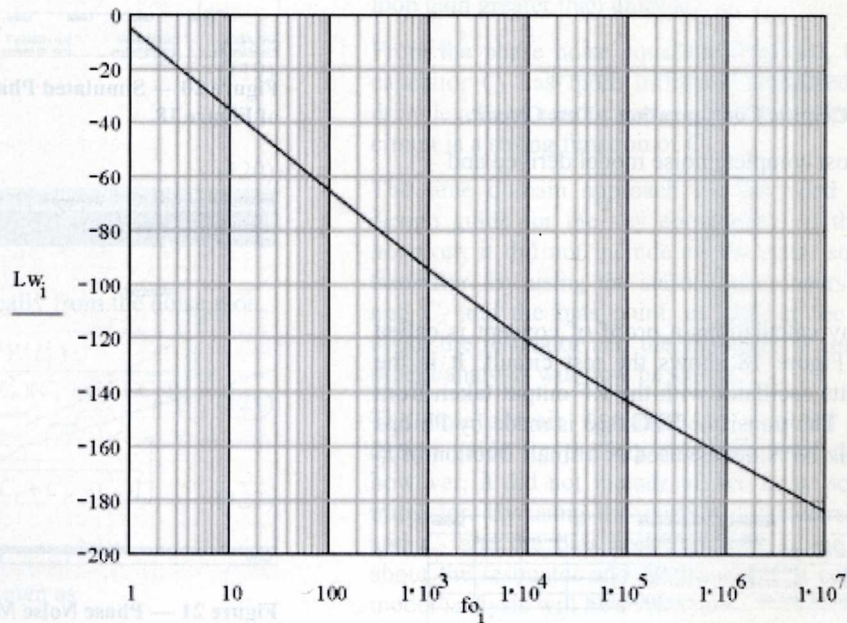


Figure 22 — Mathcad Worksheet for calculated Phase Noise of a 350 MHz Colpitts Oscillator.

The MathCad worksheet, Eqn_107_350MHz.mcd file, can be found at www.arri.org/QEXfiles.

References

- [1] www.scribd.com/doc/213845621/Communication-Circuits-Clarke-Hess#scribd
- [2] rfic.eecs.berkeley.edu/~niknejad/ee242/pdf/eecs242_lect22_phasenoise.pdf.
- [3] https://en.wikipedia.org/wiki/Barkhausen_stability_criterion.
- [4] U. L. Rohde, A. K. Poddar, *The Design of Modern Microwave Oscillators*, John Wiley, 2005.
- [5] U. L. Rohde, M. Rudolph, *RF/Microwave Circuit Design for Wireless Applications*, Wiley, New York, 2013.
- [6] Agilent Phase Noise Measurement Solution (www.home.agilent.com/agilent/application)
- [7] R. G. Rogers, *Low Phase Noise Microwave Oscillator Design*, Artech House, Inc. 1991.
- [8] Enrico Rubiola, "Phase Noise and Frequency Stability in Oscillators", Cambridge University Press, 2010.
- [9] U. L. Rohde and A. K. Poddar, "An Analytical Approach of Minimizing VCO Phase Noise," Asia-Pacific Microwave Conference, China, December 4-7, 2005.
- [10] U. L. Rohde and A. K. Poddar, "Noise Minimization Techniques for RF & MW Signal Sources (Oscillators/VCOs)", *Microwave Journal*, Sept. 2007.
- [11] U. L. Rohde and A. K. Poddar, "Techniques Minimize the Phase Noise in Crystal Oscillators", 2012 IEEE FCS, pp. 01-07, May 2012.
- [12] Marvin E. Frerking, *Crystal Oscillator Design and Temperature Compensation*, Van Nostrand Reinhold Company ISBN: 0-442-22459-1
- [13] Brendon Bentley, "An Investigation into the Phase Noise of Quartz Crystal Oscillators", MS Thesis, Stellenbosch University, March 2007.
- [14] Ajay Poddar, Ulrich Rohde, Anisha Apte, "How Low Can They Go, Oscillator Phase noise model, Theoretical, Experimental Validation, and Phase Noise Measurements", *IEEE Microwave Magazine*, Vol. 14, No. 6, pp. 50-72, Sep/Oct 2013.
- [15] Ulrich Rohde, Ajay Poddar, Anisha Apte, "Getting Its Measure", *IEEE Microwave Magazine*, Vol. 14, No. 6, pp. 73-86, Sep/Oct 2013.
- [16] Grant Moulton, "Analysis and Prediction of Phase Noise in Resonators and Oscillators", Hewlett Packard, (citeseerx.ist.psu.edu/viewdoc/download?doi=10.1.1.309.5449&rep=rep1&type=pdf).
- [17] www.ieee-uffc.org/frequency-control/learning/pdf/everard.pdf.
- [18] K. Kurokawa, "Noise in Synchronized Oscillators," *IEEE Trans. on MTT*, Vol. 16, pp. 234-240, Ap 1968.
- [19] V. Rizzoli, F. Mastri, C. Cecchefti, "Computer-Aided Noise Analysis of MESFET and HEMT Mixers," *IEEE Trans. Microwave Theory and Techniques*, Vol. MTT-37, pp 1401-1410, Sep 1989.
- [20] A. Apte, V. Madhavan, A. Poddar, U. Rohde, T. Itoh, "A Novel Low Phase Noise X-band Oscillator", *IEEE BenMAS 2014*, Drexel Univ., Philadelphia.

The IEEE Microwave Theory and Techniques Society (MTT-S) awarded the 2016 Microwave Application Award to Dr. Ulrich L. Rohde, NIUL / DJ2LR, for

"Significant contributions to the development of low-noise oscillators".

The Microwave Application Award recognizes an individual, or a team, for an outstanding application of microwave theory and techniques, which has been reduced to practice nominally 10 years before the award.